Keysight Technologies
On Determining Critical Stresses in Semiconductors: A Case Study on ZnO Crystal and GaN Freestanding Film

Application Note

Introduction

Wide band-gap semiconductors, such as zinc oxide (ZnO) and gallium nitride (GaN) are getting a lot of attention for their applications in optoelectronic and power devices. Single crystal GaN, a III-V wide band-gap semiconductor, has received a great deal of attention in the recent past due to its potential for the realization of photonic devices such as laser and light emitting diodes (LEDs) operating in the ultraviolet portion of the electromagnetic spectrum as well as solar-blind photo-detectors.[1] Its wide band-gap, high breakdown field, and high electron saturation velocity also make it an attractive candidate for the development of electronic devices operating at high temperatures, high power, and high frequency relative to competing materials such as silicon and gallium arsenide.[2,3] While GaN holds the promise for the advancement of a number of technologies, its ascension to maturity has been rather sluggish. Technological hurdles in the growth of bulk GaN by standard melt techniques and the nonexistence of a suitable lattice-matched substrate, have forced researchers to conduct the vast majority of studies in this material on heteroepitaxially grown thin films, with C-plane (0001) sapphire and silicon carbide being the traditional substrates of choice.[4] The mismatch of lattice constants and thermal expansion coefficients in such heteroepitaxy results in high dislocation densities and a high level of post-growth residual strain in the GaN film, which inevitably affects its physical properties.

Similarly, single crystal ZnO - a II-VI wide band-gap semiconductor - has received a good amount of attention in the recent past due to its potential application in short wavelength optoelectronic devices due to some advantages over the more popular GaN.[5] For example, ZnO has a simpler crystal growth technology, which translates to a lower cost material. ZnO can also be easily etched in acids and alkalis, providing an opportunity of fabrication of small-scale devices. Recently, ZnO has shown potential for applications in transparent thin-film transistors as well.6 In all cases, it is of great interest to understand the mechanical properties at the device length scales for improvements in manufacturing processes as well as better functional reliability.

In recent years, with the advent of the nanoindentation technique, there have been some efforts to determine the elastic modulus and hardness of semiconductor single crystals and thin films. However, most of these studies have been limited to determining the elastic modulus and hardness. Very little is known about the elastic to plastic transition behavior and how the defect distribution in the crystal affects the critical failure stresses. In this application note, we discuss a nanoindentation method using spherical indentation probes to characterize the elastic-plastic transition behavior and determine critical failure stresses in ZnO and GaN single crystals with (0001) orientation. Nanoindentation using a spherical probe results in an extended elastic deformation regime, and a gradual transition to elastic-plastic deformation, to enable the characterization of critical failure stresses.

Experimental

The nanoindentation experiments were carried out in a Nanoindenter G200 using spherical diamond probes with tip radii 1 and 13.5 µm. Note that the radius of the tip was verified by imaging the probes in a scanning electron microscope. The continuous stiffness measurement (CSM) attachment was used to measure the contact stiffness as a continuous function of indentation depth. The measured load (P), displacement (ht) and contact harmonic stiffness (S) were then analyzed according to Hertzian contact mechanics, as discussed below. The schematic of a spherical indentation process is shown in Fig. 1.

The contact depth (h_C) is calculated according to the Oliver-Pharr model:[7]

$$h_c = h_t - \varepsilon \frac{P}{S} \quad (1)$$

where, ε is a constant with a value of 0.75 for a spherical indenter. It is important to

KEYSIGHT TECHNOLOGIES

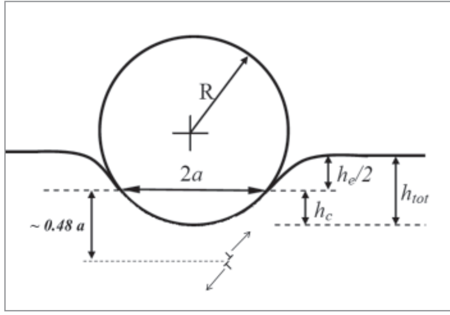

Figure 1. Schematic of spherical indentation. The labels indicate parameters those are defined in the text.

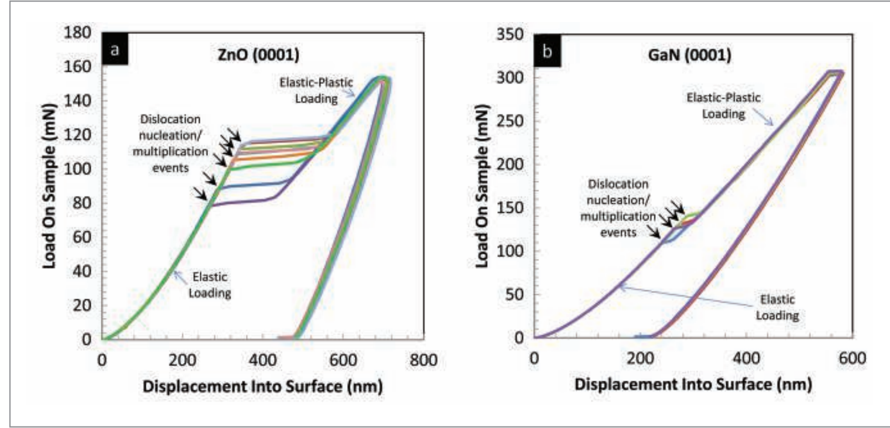

Figure 2. Nanoindentation load-displacement response of (a) ZnO (0001) crystal, and (b) GaN (0001) freestanding film, obtained using a spherical indenter of 13.5µm tip radius. Note the distinct stochastic pop-in events marked by arrows.

note here that this equation can be applied in both elastic and elastic-plastic regimes to calculate the contact depth. Once the contact depth is known, the contact radius (a) can be derived as:

$$a = \sqrt{2Rh_c - h_c^2} \quad (2)$$

where, R is the tip radius. According to the theory of elastic contacts, the contact radius is related to the harmonic contact stiffness by:[8]

$$S = 2E^*a \quad (3)$$

where, E* is the reduced modulus that is a function of both the sample and the tip, and can be expressed as:[8]

$$\frac{1}{E^*} = \frac{1-\nu^2}{E} + \frac{1-\nu_i^2}{E_i} \quad (4)$$

E and ν are Young's modulus and Poisson's ratio, respectively. The subscript 'i' represents the properties of the diamond tip, which has a Young's modulus of 1140 GPa, and a Poisson's ratio of 0.07. Hence, for the elastic regime, the modulus of the sample can be measured from the slope of an S vs. a curve, which should be linear based on the relationship mentioned in Eqn. 3.

Now, the indentation stress can be defined as:[9]

$$\sigma = \frac{P}{\pi a^2} \quad (5)$$

A definition of 'indentation strain' has also been proposed by Tabor as:[9]

$$\varepsilon = \frac{a}{R} \quad (6)$$

In the elastic regime, the indentation stress is a linear function of the indentation strain.[8]

$$\frac{P}{\pi a^2} = \frac{4}{3\pi}E^*\left(\frac{a}{R}\right) \quad (7)$$

Note here that although this expression is used here as a representative strain, a proper expression of strain, especially for elastic-plastic indentation, is still very much a topic of ongoing discussion.

Results and Discussion

Nanoindentation load-displacement results for the ZnO crystal with (0001) orientation – referred from now on as ZnO-C – obtained with the 13.5µm indenter are shown in Fig. 2a; those for the GaN freestanding film with (0001) orientation – referred as GaN-C – are shown in Fig. 2b. The pop-in events, marked by arrows in Fig. 2, are clearly evident for both ZnO-C and GaN-C. Before the discussion on the critical stresses during pop-ins, it is important to characterize the elastic modulus of the semiconducting materials to validate the accuracy of this spherical nanoindentation method.

As noted in literature, the pop-in events during contact loading of crystalline solids represent the transition from elastic to plastic deformation.[10–12] Hence, in order to measure the elastic modulus, the harmonic contact stiffness is plotted as a function of the contact radii in Fig. 3 for the data obtained prior to the pop-in events. According to Eqn. 3, the reduced modulus can be obtained from the linear slope, and thus the elastic modulus can be calculated as per Eqn. 4. The excellent linearity of the S vs. a curves for both ZnO and GaN is noteworthy, and indicates accuracy of the contact radius calculation. At 125 ± 3 GPa, the elastic modulus for ZnO-C from Fig. 3a is in excellent agreement to the Young's modulus reported in literature.[13] This value is also in reasonably good agreement with the elastic modulus determined from Berkovich nanoindentation (135 ± 3 GPa). Similarly, the elastic modulus for GaN-C is calculated from the S vs. a plot (Fig. 3b) to be 221 ± 3 GPa. The Berkovich

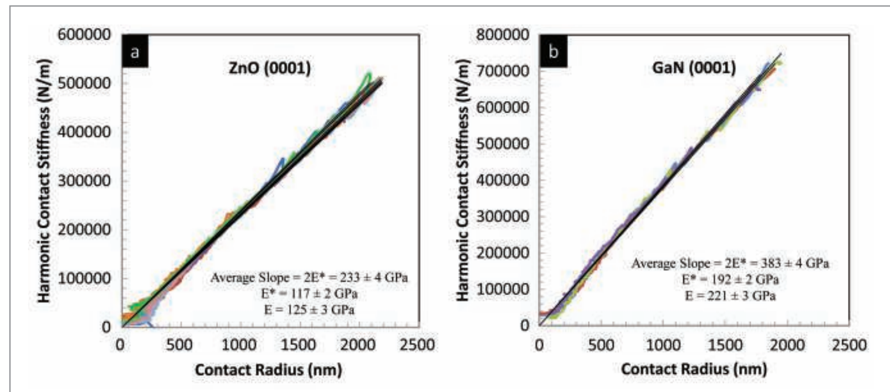

Figure 3. Harmonic contact stiffness, measured by continuous stiffness measurement, as a function of contact radius, for (a) ZnO (0001) crystal, and (b) GaN (0001) freestanding film, indented with a 13.5 µm spherical indenter.

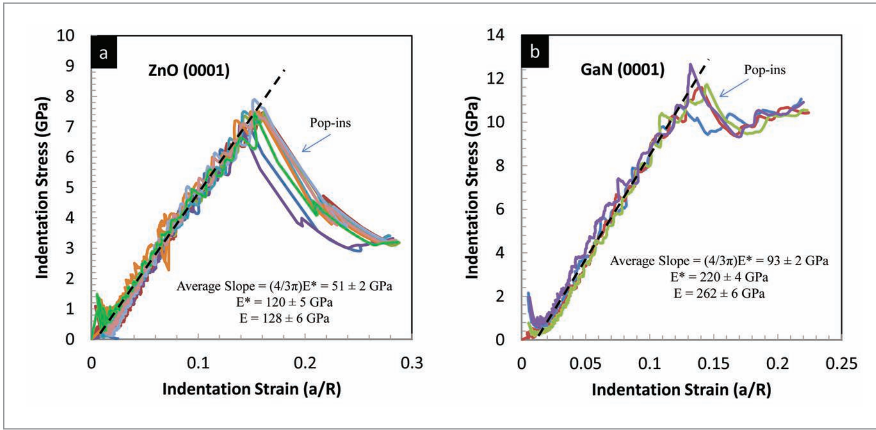

Figure 4. Indentation stress-strain curves for (a) ZnO (0001) crystal, and (b) GaN (0001) freestanding film, indented using a 13.5 µm spherical tip.

nanoindentation modulus, measured on the same surface, is reasonably close at 261 ± 3GPa.

The other way to characterize the elastic deformation is to calculate the indentation stress and strain values, according to Eqns. 5 and 6. The indentation stress-strain curves for the ZnO-C and GaN-C are shown in Figs. 4a and 4b, respectively. The slope of the elastic region before the pop-ins was used to calculate the elastic moduli, according to the Eqn. 7. The elastic modulus of both ZnO-C and GaN-C calculated in this way (shown in Fig. 4) matches well with the other measurements mentioned before – putting more credence into the methodology discussed here. It is interesting to note here that there is a great amount of scatter in the modulus values for semiconducting crystals and films reported in literature, mostly due to various processing parameters. So, even if our values are within that range it was not possible to compare it to any particular reported number. This variation is again reiterating the importance to measuring the mechanical properties of these semiconductor films and crystals for more reliable performance of the devices.

It has been discussed in literature that pop-in events during contact loading in crystalline solids represent the transition from fully elastic to elastic-plastic deformation.[14] For semiconducting ZnO and GaN, such events are related to dislocation nucleation and/or dislocation multiplication events.[11,12] It is known that the growth processes for semiconducting crystals and films often introduce point and line defects, which act as sources for dislocations during any contact loading during the manufacturing and handling. Depending on the processing parameters these inherent defects are statistically distributed in the crystals and films at different length scales.

As evident from the distribution of the pop-in loads in Figs. 2a and 2b, these defects in the ZnO-C crystal and the GaN-C film are distributed stochastically in the material, and act as dislocation sources when a critical shear stress is reached. The maximum shear stress underneath the indenter can be written as:[8]

$$\tau = 0.31\left(\frac{6PE^{*2}}{\pi^3 R^2}\right)^{\frac{1}{3}} \tag{8}$$

The maximum shear stress occurs at a depth of about 0.48 times the contact radius under the contact surface. When the maximum shear stress reaches a critical value a new dislocation pair generates from this location, as shown in the schematic in Fig. 1. Theoretical calculations for defect free crystals have proposed this value to be close to G/2π, where G is the shear modulus of the material. From the maximum shear stresses those were calculated for indents made with 1 and 13.5 µm indenters at different locations (Fig. 5), we can reasonably draw the following inferences. First, the critical shear stresses for both the ZnO-C and the GaN-C samples are lower than the theoretical predictions, suggesting that there were inherent defects in both materials that worked as dislocation sources at significantly lower stresses. Second, there is a stochastic distribution of maximum shear stresses where the pop-in, or dislocation burst, happens.

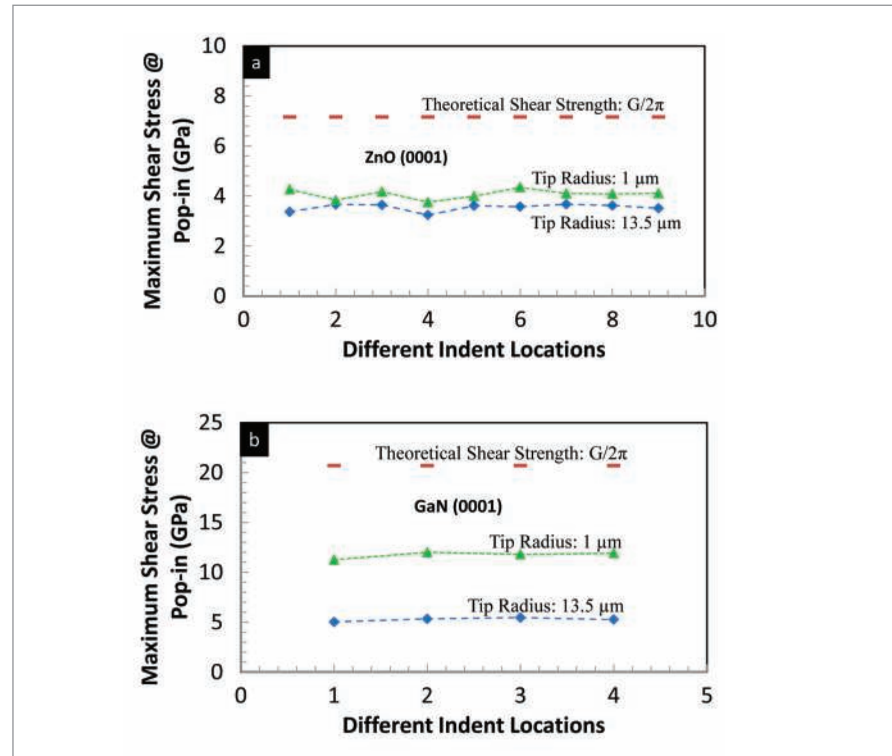

Figure 5. The maximum shear stresses at pop-in loads for different locations in (a) ZnO (0001) crystal, and (b) GaN (0001) freestanding film, plotted along with the theoretical shear strength of the corresponding materials.

This indicates that the dislocation sources are statistically distributed in the crystals – some being close and some being far away from the point of maximum shear under the indenter. Lastly, the critical stresses during pop-ins for 1 µm indents are higher compared to 13.5 µm indents. This difference indicates the length scale of defect distribution inside the crystals. The smaller the indenter tip radius the higher the critical pop-in stress as the probability of finding a dislocation source decreased under the indenter. Hence, statistical analysis of critical pop-in stresses with different size spherical indenters can be powerful tool to analyze the distribution of defects those form during the manufacturing processes of these semiconducting materials.

Summary and Conclusions

The Nanoindenter G200 was used to perform spherical nanoindentation experiments on ZnO single crystal and GaN freestanding film. The load, displacement and contact stiffness data were utilized to calculate the elastic properties of the semiconducting materials. The critical deformation stresses — as indicated by distinct pop-in events during nanoindentation — were determined for both samples. Understanding these critical contact stresses help in characterizing the defect distribution in these semiconducting materials, which in turn will be beneficial for their manufacturing processes and for designing devices with better functional reliability.

Nanomeasurement Systems from Keysight Technologies

Keysight Technologies, the premier measurement company, offers high-precision, modular nanomeasurement solutions for research, industry, and education. Exceptional worldwide support is provided by experienced application scientists and technical service personnel. Keysight's leading-edge R&D laboratories ensure the continued, timely introduction and optimization of innovative, easy-to-use nanomeasure system technologies.

www.keysight.com/find/nano

References

1. Pearton, S.J., Zolper, J.C., Shul, R.J., Ren, F. GaN: Processing, defects and devices. *J. App. Phys.* 86, 1–78 (1999).
2. Pearton, S.J. et al. GaN electronics for high power, high temperature applications. *Materials Science and Engineering* B 82, 227–231 (2001).
3. Oxley, C.H. Gallium Nitride: The promise of high RF power and low microwave noise performance in S and I band. *Solid-state Electronics* 48, 1197–1203 (2004).
4. Liu, L., Edgar, J.H. Substrates for gallium nitride epitaxy. *Materials Science and Engineering R* 37, 61–127 (2002).
5. Kucheyev, S.O., Bradby, J.E., Williams, J.S., Jagadish, C., Swain, M.V. Mechanical deformation of single-crystal ZnO. *App. Phys. Lett* 80, 956–958 (2002).
6. Ozgur, U. et al. A comprehensive review of ZnO materials and devices. J. *App. Phys.* 98, 041301 (2005).
7. Oliver, W.C., Pharr, G.M. An improved technique for determining hardness and elastic modulus using load and displacement sensing indentation experiments. *Journal of Materials Research* 7, 1564–1583, doi:doi:10.1557/JMR.1992.1564 (1992).
8. Johnson, K.L. *Contact Mechanics*. (Cambridge University Press, 1987).
9. Tabor, D. *The hardness of metals.* (Oxford University Press).
10. Lorenz, D. et al. Pop-in effect as homogeneous nucleation of dislocations during nanoindentation. *Physical Review B* 67, 172101 (2003).
11. Basu, S., Barsoum, M.W. Deformation micromechanisms of ZnO single crystals as determined from spherical nanoindentation stress–strain curves. *Journal of Materials Research* 22, 2470–2477, doi:doi:10.1557/jmr.2007.0305 (2007).
12. Basu, S., Barsoum, M.W., Williams, A.D., Moustakas, T.D. Spherical nanoindentation and deformation mechanisms in freestanding GaN films. J*ournal of Applied Physics* 101, 083522, doi:doi:http://dx.doi.org/10.1063/1.2719016 (2007).
13. Gadzhiev, G.G. The Thermal and Elastic Properties of Zinc Oxide-Based Ceramics at High Temperatures. *High Temperature* 41, 778–782, doi:10.1023/b:hite.0000008333.59304.58 (2003).
14. Bei, H., George, E.P., Hay, J.L., Pharr, G.M. Influence of Indenter Tip Geometry on Elastic Deformation during Nanoindentation. *Physical Review Letters* 95, 045501 (2005).

KEYSIGHT TECHNOLOGIES

This information is subject to change without notice.
© Keysight Technologies, 2013 - 2014
Published in USA, August 3, 2014
5991-3469EN
www.keysight.com